
Article:
Braun, H.P., Mehmood, A., Hovhannisyan, M. et al. (8 more authors) (2017) Microwave properties and structure of La–Ti–Si–B–O glass-ceramics for applications in GHz electronics. Journal of the European Ceramic Society, 37 (5). pp. 2137-2142. ISSN 0955-2219

https://doi.org/10.1016/j.jeurceramsoc.2016.11.048

Microwave properties and structure of La-Ti-Si-B-O glass-ceramics for applications in GHz electronics

Hubertus P. Braun[a,b,c,*], Arshad Mehmood[d], Martun Hovhannisyan[c], Huairuo Zhang[e], Damoun Sohrabi Baba Heidary[f,g], Clive Randall[f,g], Michael T. Lanagan[f,g], Rolf Jakoby[d], Ian M. Reaney[e], Martin Letz[c], Hans-Joachim Elmers[a,b]

[a] *Institut für Physik, Johannes Gutenberg-Universität Mainz, Staudingerweg 7, 55128 Mainz, Germany*
[b] *Graduate School Materials Science in Mainz, Staudinger Weg 9, 55128 Mainz, Germany*
[c] *SCHOTT AG, Hattenbergstrasse 10, 55122 Mainz, Germany*
[d] *Institute for Microwave Engineering and Photonics, Technical University of Darmstadt, Merckstrae 25, 64283 Darmstadt, Germany*
[e] *Department of Materials Science and Engineering, University of Sheffield, Sir Robert Hadfield Building, Mappin Street, Sheffield S1 3JD, United Kingdom*
[f] *Department of Materials Science & Engineering, The Pennsylvania State University, University Park, PA 16802, USA*
[g] *Center for Dielectrics & Piezoelectrics, Materials Research Institute, The Pennsylvania State University, University Park, PA 16802, USA*

Abstract

A castable, dielectric bulk glass-ceramic material of the La_2O_3-TiO_2-SiO_2-B_2O_3 system is developed which is able to fulfill the requirements for dielectric loading-based mobile communication technologies ($\varepsilon_r > 20$, $Qf > 5000$ GHz, $|\tau_f| < 20$ ppm/K; at GHz frequencies). It is shown that the given dielectric requirements can be fulfilled by glass-ceramic materials without being dependent on complex ceramic processing techniques which intrinsically lead to unfavorable structural properties (porosity, inhomogeneity, non-uniformity). Depending on the heat treatment during the ceramming process, the material exhibited permittivity values of $20 < \varepsilon_r < 30$, quality factor 2000 GHz $< Qf <$ 10000 GHz and a temperature coefficient of resonance frequency -100 $< \tau_f <$ +180 ppm/K. A zero τ_f material with a Qf value of 9500 GHz and $\varepsilon_r = 21.4$ could be achieved at a ceramming temperature $T_{\mathrm{cer}} = 870$ °C. The material is aimed to provide an

*Corresponding author now at: Robert Bosch GmbH, Postfach 30 02 20, 70442 Stuttgart, Germany
Email address: h.braun86@gmx.de (Hubertus P. Braun)

alternative to existing, commercially used sintered ceramic materials. Further focus is laid on the investigation of the dominant dielectric loss mechanisms in the GHz frequency range and how they are correlated with the microstructure.
Keywords: dielectric glass-ceramics, titanate-based glass-ceramics, microwave materials, GHz materials, dielectric-loaded antenna materials

1. Introduction

Dielectric oxide ceramics have revolutionized the microwave wireless communication industry by reducing size and cost of filter, resonator and antenna components in various applications ranging from cellular phones to global positioning systems [1]. This is apparent by the increasing number of smart phones combining the use of multiple microelectronic components of different operating frequencies on a limited spatial area (GSM/UMTS/LTE, GPS, WLAN, Bluetooth). Miniaturization is a critical factor for hand-held devices and can be directly observed in the decrease of size and weight of the devices in recent years. The required performance increase for future technologies (e.g. 5G) can be achieved by the use of MIMO-based antenna systems [2]. Miniaturization and MIMO can be realized by the use of dielectric loading-based implementation solutions. While for cavity filters, exceptionally low-loss materials ($Qf >$ 100000 GHz) are necessary [3], dielectric loading-based wireless communication technologies (MIMO, GPS, multiresonant dielectric resonator antennas) as for example dielectrically loaded antennas (DLA) can utilize dielectrics with higher losses ($Qf > 5000$ GHz, $\varepsilon_r > 20$, $|\tau_f| < 20$ ppm/K), as their antenna efficiency is mainly dominated by metallization losses [4]. A quite large number of commercially available ceramics with excellent dielectric properties already exists [3], but due to their manufacturing process (sintering) they show some disadvantageous non-electronic properties which cause problems for their use in DLA applications [5, 6]:

- porosity (problematic for metallization processes)
- blank inhomogeneity/non-uniformity (performance deterioration)

- batch-to-batch variation of the dielectric properties ($\Delta\varepsilon_r/\varepsilon_r \approx$ 1-2 %)

At low frequency ranges dielectric resonators become larger which intensifies these manufacturing-related problems. Especially for the frequency range below 2 GHz, which is important for mobile communications large blank geometries are necessary [7]. For these applications glass-ceramic materials can be a suitable alternative to sintered ceramic materials. Glass-ceramic-based dielectrics tend to have comparatively higher dielectric losses due to the residual glassy phase, but provide superior structural properties to sintered ceramics. As glass-ceramics are initially produced from a homogeneous liquid glass melt, they are intrinsically pore-free and provide a better material homogeneity and reproducibility. First work on glass-ceramic-based dielectrics for DLA applications was made in the Bi_2O_3-Nb_2O_5-SiO_2-B_2O_3 system by Mirsaneh et al. [8, 4], but the dielectric requirements could not be sufficiently fulfilled. In this work the development of a dielectric glass-ceramic material with suitable dielectric properties (Qf = 9500 GHz, ε_r = 21.4, τ_f = -1 ppm/K) is presented.

2. Material development and characterization

2.1. Motivation for the choice of the La_2O_3-TiO_2-SiO_2-B_2O_3 system

The dielectric properties of glass-ceramic material system dominantly determined by the dielectric properties of the existing crystalline phases, which were investigated in literature (e.g. [1]) under consideration of the requirements of the aimed application ($\varepsilon_r > 20$, $Qf > 5000$ GHz and $|\tau_f| \leq 20$ ppm/K). In the ternary system La_2O_3-TiO_2-SiO_2, two optimal crystalline phases ($La_4Ti_9O_{24}$ and $La_2Ti_2SiO_9$, see Tab. 1) exist, which show sufficiently high ε_r and Qf, in combination with a small positive τ_f. The τ_f values are optimal for the use in glass-ceramic materials, as the residual glassy phase generally has a negative τ_f [1, 9] and both phases can thereby compensate to an overall τ_f close to zero. TiO_2 (rutile) and $LaBO_3$ are minor phases (< 20 wt%) for some glass compositions/ceramming programs. TiO_2 (rutile) has excellent dielectric properties [10] but also an extremely high τ_f. $LaBO_3$ crystallizes from the excess B_2O_3

and La_2O_3 which is not used in the major crystalline phases. To enhance the glass forming ability of the system (avoid devitrification), a combination of the two network former oxides SiO_2 and B_2O_3 was added. This enables a glass composition in the field of crystallization of the two target crystalline phases. Nevertheless, the aim is always a one-crystalline-phase material with main content of $La_4Ti_9O_{24}$ or $La_2Ti_2SiO_9$, as multiple-phase materials always tend to have a higher dielectric losses [11]. Unfortunately SiO_2 and B_2O_3 only have a low ionic polarizability due to their strong covalent bonds, but also they have a comparatively low dielectric loss [12, 1]. The amount of SiO_2 and B_2O_3 was kept to a minimum to achieve a maximum amount of crystalline phase respectively minimum amount of residual glass phase content after the ceramming process.

2.2. Glass melting and ceramming process

The glass samples were melted from milled dry powders according to the batch composition inside a one litre Pt-Ir alloy crucible. The melts are cast into size-adjustable steel molds. From each melt 4 glass bars of 2 × 5 × 23 cm size could be made, which were then cut into suitable geometries for subsequent measurements. The high volume and the possibility to stir the melt ensured homogeneous samples. The melting temperature T_m varied between 1450 °C to 1650 °C. A typical melting procedure can be summarized as:

- Insertion of raw materials in 5 g steps at T_m - 100 °C (typically 1500 °C), until batch is melted
- Oxygen bubbling and stirring (to achieve oxidizing melting conditions) with 27 l/h for 30 min at T_m - 50 °C (typically 1550 °C)
- Keeping time at the high temperature chamber furnace for t_k = 30 min at T_m (typically 1600 °C)
- Casting into steel mold (on room temperature)
- Cooling in the cooling furnace to prevent crack formation (preheated at T_g - 20 °C) with 20 K/h until room temperature

First compositional attempts were made with La:Ti ratios close to the stoichiometry of the $La_4Ti_9O_{24}$ phase (e.g. sample S2, see Fig. 1). These glasses showed a strong devitrification tendency (see Fig. 2) and therefore the composition was moved closer to the stoichiometry of the $La_2Ti_2SiO_9$ phase. An important concept to stabilize glass formation in multicomponent systems is the principle of glass frustration [13]. The increase of the number of different cations/components leads to a "geometrical frustration" which increases/decreases (?) disorder of the system and thereby retards the formation of an ordered crystalline state [14], respectively stabilizes the disordered amorphous glassy phase. Fig. 1 shows a pseudo-ternary compositional diagram and a comparatively small glass-forming area. TiO_2 was partially substituted by ZrO_2 and La_2O_3 by other rare earth oxides (RE: CeO_2, Nd_2O_3, Sm_2O_3, Gd_2O_3) to create additional disorder and thereby improve the glass-forming properties of the system. A Ti substitution with 10 - 20 % Zr and a La substitution with 1 - 5 % RE showed the best results. The composition S1 (see Fig. 2) showed optimum glass-forming abilities (purely amorphous) in combination with sufficiently good dielectric properties after the ceramming process (T_g = 870 °C).

2.3. Ceramming & phase assemblage

During the ceramming process the purely amorphous sample partially crystallizes. The ceramming temperatures for the investigated system were around 800 °C to 1050 °C with the program shown in Tab. 2. The best dielectric results (high Qf & small $|\tau_f|$) were achieved for samples ceramized at comparatively low temperatures (e.g. ceramming program P1: T_{cer} = 870 °C, t_{cer} = 50 h). The dominant nucleation of the major phases ($La_4Ti_9O_{24}$, TiO_2, $La_2Ti_2SiO_9$) is caused by dissolved Pt particles which are corroded from the crucible. At higher temperatures (T_{cer} > 950 °C) also surface crystallization is observed. The Pt particles effectively nucleate $La_4Ti_9O_{24}$ as main phase at low ceramming temperatures in combination with minor amounts of an unknown lanthanum-silicate phase (approximate stoichiometry La:Si = 1:1 (identified by TEM/EELS), assumed: $La_2Si_2O_7$, but does not match with the XRD peaks) and SiO_2 as minor

phases, which are found between the dendrite branches (see Fig. 4). It is observed via TEM/EELS, that Zr partially substitutes on the Ti lattice site in the $La_4Ti_9O_{24}$ phase. Due to the unidentified peaks ($\diamond$) in the XRD diffractogram (Fig. 3), which might be caused by the lanthanum-titanate phase, no Rietveld analysis could be performed. At medium ceramming temperatures 900 °C $< T_{\mathrm{cer}} <$ 940 °C, the $La_4Ti_9O_{24}$ phase decreases and TiO_2 becomes dominant leading to a strong increase of ε_r and τ_f. High ceramming temperatures $T_{\mathrm{cer}} >$ 940 °C, favor the formation of $La_2Ti_2SiO_9$ as main crystalline phase. The excess TiO_2 and B_2O_3 form the minor phases TiO_2 (rutile needles) and $LaBO_3$ in the boundary regions between the $La_2Ti_2SiO_9$ areas. $LaBO_3$ is present in all temperature ranges as minor phase and its amount increases with increasing temperature. For $T_{\mathrm{cer}} >$ 950 °C $LaBSiO_5$ is formed probably in a reaction of the $LaBO_3$ and the SiO_2. Further small amounts of amorphous SiO_2 are found, which do not show any XRD peaks and were detected by TEM/EELS.

2.4. Dielectric properties

The dielectric properties in the GHz frequency range were measured using the Hakki-Coleman method [15] (ε_r and Qf) and the cylindrical cavity resonance technique [16, 17] (τ_f). Further electrical conductivity measurements with an impedance analyzer were made from the Hz to MHz range (see Fig. 6) to investigate the contribution of conductive losses in the GHz region.

2.4.1. Low frequency properties - electrical conductivity

The electrical conductivity of a wide class of conducting materials (including amorphous semiconductors, defect containing single crystals, polymers, ionic conductors and glasses) shows this universal frequency dependence (Eq. (1)) which is given by the phenomenological UDR model (universal dielectric response) proposed by Jonscher [18, 19, 20]

$$\sigma(f) = \sigma_{DC} + \sigma_0 f^s \quad . \tag{1}$$

The exponent s varies in the range 0.3 to 1 for different materials and the temperature dependence of σ_{DC} and σ_0 follows a thermally activated Arrhenius

type behavior. Jonscher [20] states that this model is valid up to GHz frequencies until the low frequency flank of the phonon modes starts to show contributions. The room temperature conductivity is therefore fitted by this model, shown for S1 and S1P1 in Fig. 6. The associated dielectric loss $\tan(\delta)_{\mathrm{ex}}$ (calculated via Eq. (2)) values were extrapolated to the GHz region and compared to the values measured directly by the Hakki-Coleman method.

$$\tan(\delta)(\omega) = \frac{\varepsilon_r''}{\varepsilon_r'} = \frac{\sigma(\omega)}{\omega\varepsilon_0\varepsilon_r'} \quad . \tag{2}$$

It could be shown that for glass S1 and glass-ceramic S1P1, the (extrapolated) conductive losses $\tan(\delta)_{\mathrm{ex}}$ were approximately one order of magnitude lower than the directly measured $\tan(\delta)$ values in the GHz range. The temperature dependent measurements show the expected behavior with a comparatively strong temperature dependence of the σ_{DC}-contribution. It can be seen that the conductivity at room temperature is dominated by the frequency dependent contribution and only for higher temperatures (> 200 °C) the DC contribution can not be neglected. Glass (S1) and glass-ceramic (S1P1) show a similar behavior. In Tab. 3 a comparison between the extrapolated $\tan(\delta)_{\mathrm{ex}}$ values and the ones measured in the GHz range via Hakki-Coleman is made. The conductivities of both samples are at least one order of magnitude too low to significantly contribute to the overall dielectric loss in the GHz range. The dominant loss contribution is probably caused by anharmonic interaction between the microwave photons and phonons, with main loss contributions given by two or three-phonon processes as described by Gurevich and Tagantsev [21, 22, 23].

2.4.2. Microwave properties

At low ceramming temperatures $T_{\mathrm{cer}} = 850$ - 900 °C the dielectric properties are dominated by the presence of $La_4Ti_9O_{24}$, leading to significant increase of the Qf value up to 9000 - 9500 GHz in combination with a sufficiently high $\varepsilon_r = 21.5$ - 22.5 and τ_f close to 0 ppm/K, fulfilling all dielectric requirements. From $T_{\mathrm{cer}} = 900$ - 940 °C the $La_4Ti_9O_{24}$ phase reduces and TiO_2 (rutile) starts to become the dominant phase accompanied by a large increase in permittivity

(up to $\varepsilon_r = 30$) and temperature coefficient ($\tau_f = 170$ ppm/K), whereby the Qf value reduces to approx. 7000 GHz. The high τ_f value makes this temperature region unsuitable for the given DLA requirements. Above 940 °C the $La_2Ti_2SiO_9$ becomes the dominant main phase, but due to the minor amounts of TiO_2, the τ_f values are still too large. For ceramming temperatures $T_{cer} >$ 1000 °C the Qf value even decreased further, probably due to the increasing amount of $LaBO_3$ and $LaBSiO_5$.

In Tab. 4 the most relevant ceramized samples of S1 are summarized.

3. Conclusion

A devitrification-stable basic glass in the La_2O_3-TiO_2-SiO_2-B_2O_3 system has been developed and stabilized by doping. The nucleation mechanism of Pt particles was investigated and the ceramming process was adapted for a maximum amount of the desired lanthanum-titanate crystalline phases to achieve optimum dielectric properties. The microstructure of the glass-ceramic was analyzed by SEM/TEM and XRD measurements and correlated with the macroscopic dielectric microwave properties which were characterized by GHz resonance methods. An optimum material with dielectric properties suitable for DLA applications could be realized (S1P1: $\varepsilon_r = 21.4$, $Qf = 9500$ GHz, $\tau_f =$ -1 ppm/K). The dielectric loss in the GHz range and low frequency regions (Hz to MHz) was investigated to achieve a general understanding of the dominant high frequency loss mechanisms. The evaluated dielectric properties were extrapolated from the adjacent frequency range to the GHz region, showing that the conductive loss is no major contribution of the dielectric loss in the GHz range. In conclusion, it can be summarized that within the framework of this work, the suitability of the investigated La_2O_3-TiO_2-SiO_2-B_2O_3-based glass-ceramics for the use in DLA applications was proven and the macroscopic dielectric properties could be correlated respectively modified by the control of the microstructure of the material.

Acknowledgements

H. Braun gratefully acknowledges the financial support from the MAINZ graduate school, the SCHOTT AG and S. Knöner for the fruitful discussions.

References

[1] M. T. Sebastian, Dielectric Materials for Wireless Communication, Elsevier, 2008.

[2] F. Vook, A. Ghosh, T. Thomas, MIMO and beamforming solutions for 5G technology, Microwave Symposium (IMS), 2014 IEEE MTT-S International (2014) 1–4doi:10.1109/MWSYM.2014.6848613.

[3] I. M. Reaney, D. Iddles, Microwave dielectric ceramics for resonators and filters in mobile phone networks, Journal of the American Ceramic Society 89 (7) (2006) 2063–2072.

[4] M. Mirsaneh, O. P. Leisten, B. Zalinska, I. Reaney, Bismuth niobate-based glass ceramics for dielectrically loaded microwave antennas, Functional Materials Letters 1 (1) (2008) 25–30.

[5] H. Braun, Glaskeramiken mit paraelektrischen Phasen für mobile Anwendungen im GHz Bereich, Diploma thesis, University of Mainz.

[6] H. Braun, Glass-ceramics with paraelectric phases for mobile applications in ghz electronics, PhD thesis, University of Mainz.

[7] S. Penn, N. Alford, Chapter 10 - ceramic dielectrics for microwave applications, in: H. S. Nalwa (Ed.), Handbook of Low and High Dielectric Constant Materials and Their Applications, Academic Press, Burlington, 1999, pp. 493–532. doi:http://dx.doi.org/10.1016/B978-012513905-2/50024-8.
URL http://www.sciencedirect.com/science/article/pii/B9780125139052500248

[8] M. Mirsaneh, O. P. Leisten, B. Zalinska, Circularly polarized dielectric-loaded antennas: Current technology and future challenges, Advanced Functional Materials 18 (16) (2008) 2293–2300.

[9] J. M. Wu, H.-L. Huang, Microwave properties of zinc, barium and lead borosilicate glasses, Journal of Non-Crystalline Solids 260 (1999) 116–124.

[10] S. B. Cohn, Microwave bandpass filters containing high-Q dielectric resonators, IEEE Transactions on Microwave Theory and Techniques 16 (4) (1968) 218–227.

[11] J. Takahashi, K. Kageyama, K. Kodaira, Microwave dielectric properties of lanthanide titanate ceramics, Japanese Journal of Applied Physics 32 (9B) (1993) 4327–4331.

[12] L. Navias, R. L. Green, Dielectric properties of glasses at ultra-high frequencies and their relation to composition, The Journal of the American Ceramic Society 29 (10) (1946) 267–276.

[13] D. Kivelson, S. Kivelson, X. Zhao, Z. Nussinov, G. Tarjus, A thermodynamic theory of supercooled liquids, Physica A: Statistical Mechanics and its Applications 219 (1) (1995) 27–38.
URL http://EconPapers.repec.org/RePEc:eee:phsmap:v:219:y:1995:i:1:p:27-38

[14] J. Zarzycki (Ed.), Halide Glasses, in: [Materials science and technology]: Glasses and amorphous materials, Vol. 9. Glasses and amorphous materials, VCH, Weinheim [u.a.], 1991, literaturangaben.
URL http://www.ulb.tu-darmstadt.de/tocs/16845870.pdf

[15] B. W. Hakki, P. D. Coleman, A dielectric resonator method of measuring inductive capacities in the millimeter range, IRE Transactions on Microwave Theory and Techniques 8 (4) (1960) 402–410.

[16] J. Sheen, Study of microwave dielectric properties by various resonance techniques, Measurement 37 (2) (2005) 123–130.

[17] J. Sheen, Comparisons of microwave dielectric property measurements by transmission reflection techniques and resonance techniques, Measurement Science and Technology 20 (4) (2009) 12pp.

[18] A. K. Jonscher, Dielectric relaxation in solids, Journal of Physics D: Applied Physics 32 (14) (1999) R57.
URL http://stacks.iop.org/0022-3727/32/i=14/a=201

[19] A. K. Jonscher, A new understanding of the dielectric relaxation of solids, Journal of Materials Science 16 (8) (1981) 2037–2060. doi:10.1007/BF00542364.
URL http://dx.doi.org/10.1007/BF00542364

[20] A. K. Jonscher, The universal dielectric response, Nature 267 (1977) 673–679.

[21] V. L. Gurevich, A. K. Tagantsev, Intrinsic dielectric loss in crystals, Advances in Physics 40 (6) (1991) 719–767. arXiv:http://dx.doi.org/10.1080/00018739100101552, doi:10.1080/00018739100101552.
URL http://dx.doi.org/10.1080/00018739100101552

[22] A. K. Tagantsev, J. Petzelt, N. Setter, Relation between intrinsic microwave and submillimeter losses and permitivity in dielectrics, Solid State Communications 87 (12) (1993) 1117 – 1120. doi:http://dx.doi.org/10.1016/0038-1098(93)90812-2.
URL http://www.sciencedirect.com/science/article/pii/0038109893908122

[23] A. K. Tagantsev, Phonon mechanisms of intrinsic dielectric loss in crystals, in: N. Setter, E. Colla (Eds.), Ferroelectric Ceramics, Monte Verit, Birkhäuser Basel, 1993, pp. 127–145. doi:10.1007/978-3-0348-7551-6_4.
URL http://dx.doi.org/10.1007/978-3-0348-7551-6_4

[24] Y. Liu, P. Lin, Effects of glass additions on microwave dielectric properties of $La_4Ti_9O_{24}$ ceramics, Materials Chemistry and Physics 92 (1) (2005) 98–103.

[25] S. Thomas, B. Sayoojyam, M. T. Sebastian, Microwave dielectric properties of novel rare earth based silicates: $RE_2Ti_2SiO_9$, Journal of Materials Science: Materials in Electronics 22 (2011) 1340–1345.

[26] M. Maeda, T. Yamamura, T. Ikeda, Dielectric characteristics of several complex oxide ceramics at microwave frequencies, Japanese Journal of Applied Physics 26 (2) (1987) 76–79.

[27] T. Takada, K. Kageyama, Synthesis and microwave dielectric properties of La_2O_3-xB_2O_3-based melt mixtures for low-temperature cofired ceramics, Japanese Journal of Applied Physics 44 (9A) (2005) 6629–6635.

[28] T. Takada, H. Yamamoto, K. Kageyama, Synthesis and microwave dielectric properties of xRe_2O_3-yB_2O_3 (Re:La,Nd,Sm,Dy,Ho,Y) compounds, Japan Society of Applied Physics 42 (9B) (2003) 6162–6167.

[29] M. Janezic, Nondestructive relative permittivity and loss tangent measurements using a split-cylinder resonator, Ph.D. thesis, University of Colorado (2003).

Phase	ε_r	Qf[GHz](f_{meas})	τ_f[ppm/K]	Ref.	JCPDS(ICCD)
$La_4Ti_9O_{24}$	37	24800(8 GHz)	+15	[24, 11]	00-036-0137
$La_2Ti_2SiO_9$	28	29500(5 GHz)	+23	[25]	01-082-1490
TiO_2(Rutile)	104	44000(4 GHz)	+450	[26, 1]	01-086-0148
$LaBO_3$	12.5	53000(12 GHz)	N/A	[27, 28]	00-012-0762
$LaSiBO_5$	N/A	N/A	N/A	N/A	01-077-0989
SiO_2(glass)	3.8	67000(9 GHz)	< 0	[29]	

Table 1: Microwave properties and JCPDS code for the relevant crystal phases in the La_2O_3-TiO_2-SiO_2-B_2O_3 system

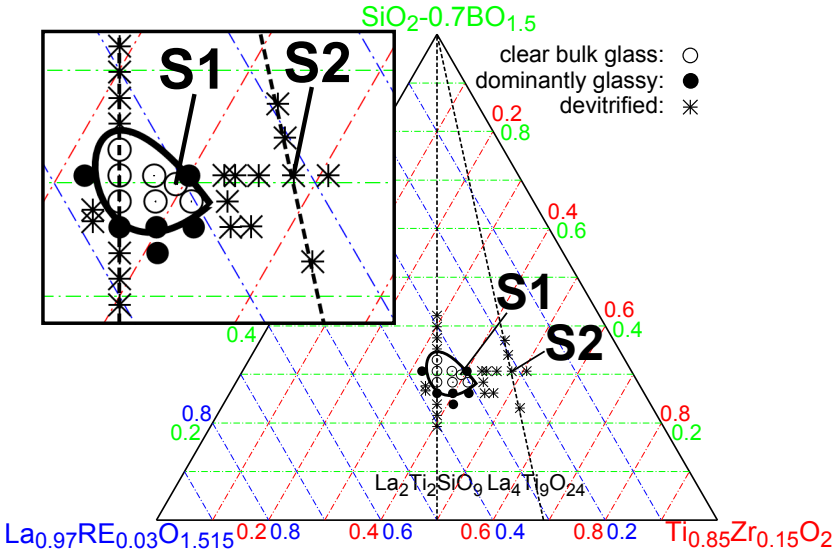

Figure 1: Pseudo-ternary diagram to visualize the glass-forming area, the black dashed lines correspond to La:Ti ratios of 1:1 ($La_2Ti_2SiO_9$) resp. 4:9 ($La_4Ti_9O_{24}$)

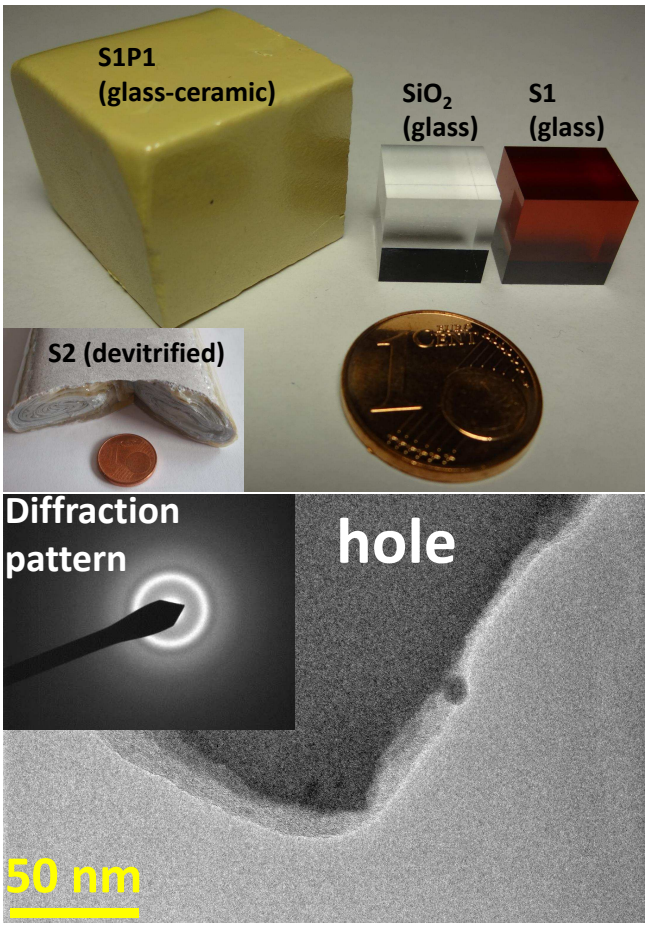

Figure 2: Top picture: left: ceramized glass S1P1 (P1: T_{cer}= 870 °C, t_{cer}= 50 h, see Tab. 2), middle: commercial SiO_2 glass, right: glass S1, bottom left: devitrified glass S2, bottom picture: TEM image and diffraction pattern of glass S1, showing a purely amorphous sample

R1	Z1	H1	R2	Z2	H2	R3	Z3	H3	R4	Z4
200	T_{cer}	t_{cer}	40	750	0	20	550	0	40	20

Table 2: Typical ceramming program (Abbr.: R: Rate [K/h], Z: holding temperature [°C], H: holding time [h])

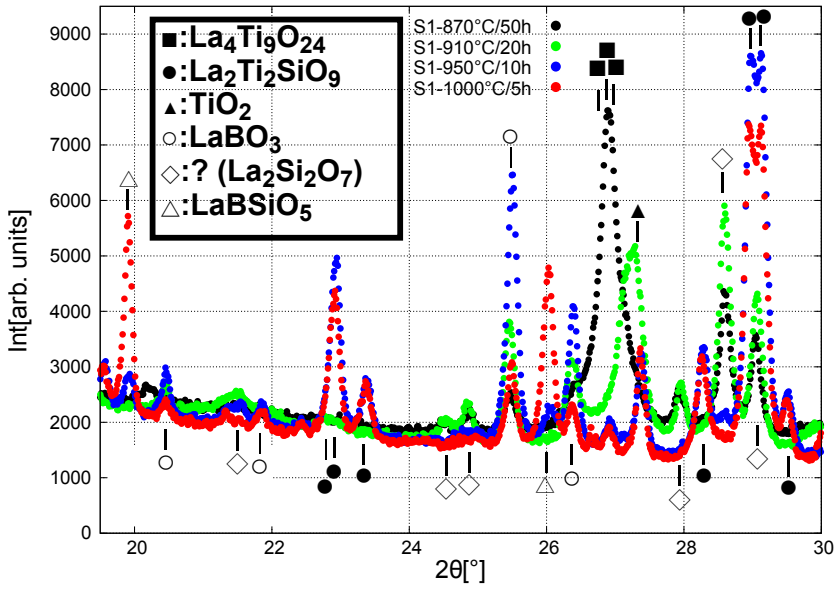

Figure 3: XRD diffractogram of S1 ceramized at different $T_{\mathrm{cer}}/t_{\mathrm{cer}}$ (the peaks marked with $\diamond$ could not be assigned and also do not correspond to the $La_2Si_2O_7$ phase, which was detected by TEM/EELS measurements but not seen in the XRD, see Fig. 5)

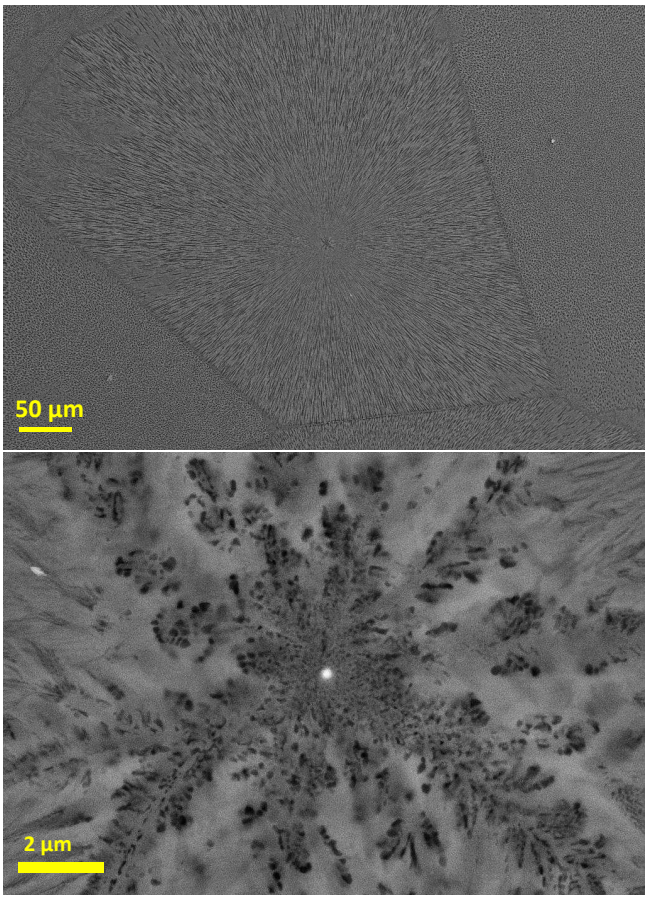

Figure 4: Top: SEM magnification of S1P1 showing a dendritic crystal growth induced by Pt, bottom: Pt particle as nucleus in the center of the crystal

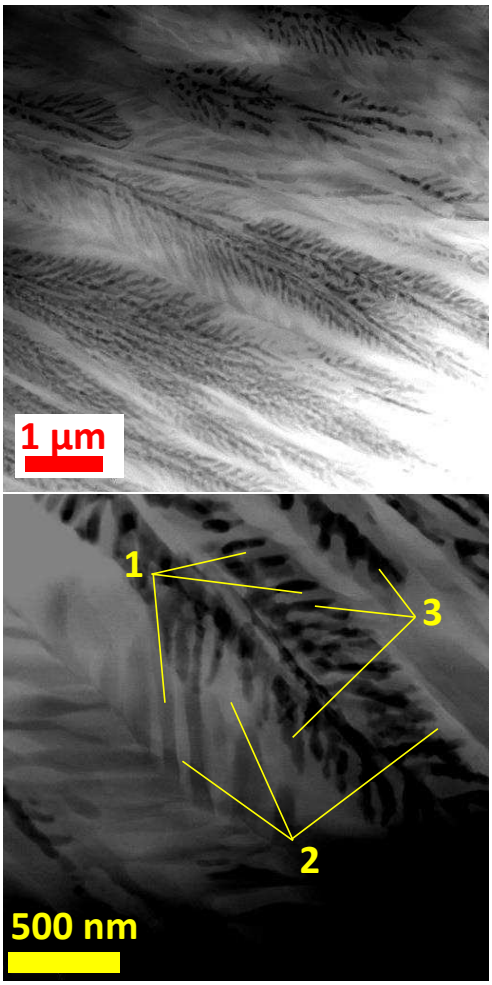

Figure 5: Dark field TEM image of S1P1 (dendrite growth direction parallel to the image plane, phases identified via TEM/EELS: 1: $La_4(Ti_{1-\delta}Zr_\delta)_9O_{24}$ ($\delta \approx 0.1$-0.2), 2: $La_2Si_2O_7$, 3: amorphous SiO_2)

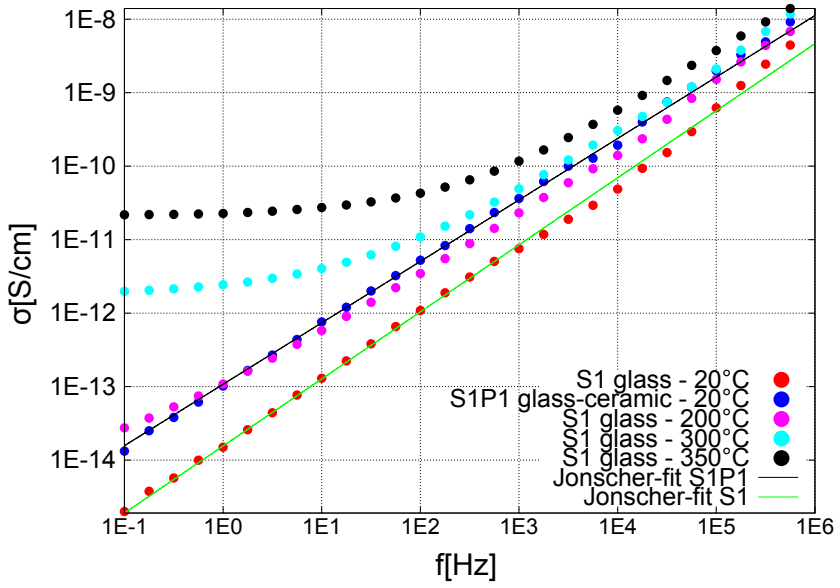

Figure 6: Electrical conductivity in dependence of frequency (The room temperature values of S1 and S1P1 are fitted with the Jonscher model to show the consistency with Eq. (1)

Sample	f[GHz]	ε_r	$\tan(\delta)$	σ_0	s	σ_{ex}[S/cm]	$\tan(\delta)_{\mathrm{ex}}$	q[%]
S1	10.57	20.4	5.76	$1.56{\cdot}10^{-14}$	0.91	$2.2{\cdot}10^{-5}$	0.18	3.2
S1P1	10.42	21.4	1.1	$1.08{\cdot}10^{-13}$	0.84	$2.6\cdot10^{-5}$	0.16	18.8

Table 3: Extrapolation of the conductivity loss contribution to the GHz frequency range by using the Jonscher model (whereby $\sigma_{\mathrm{DC}} \approx 0$ for both samples, $q = \tan(\delta)_{\mathrm{ex}}/\tan(\delta)$ (ex: extrapolated), $\tan(\delta)_{(\mathrm{ex})}$ values given in 10^{-3} and σ_0 in S/cm Hz^{-s} (not shown above due to the lack of space)

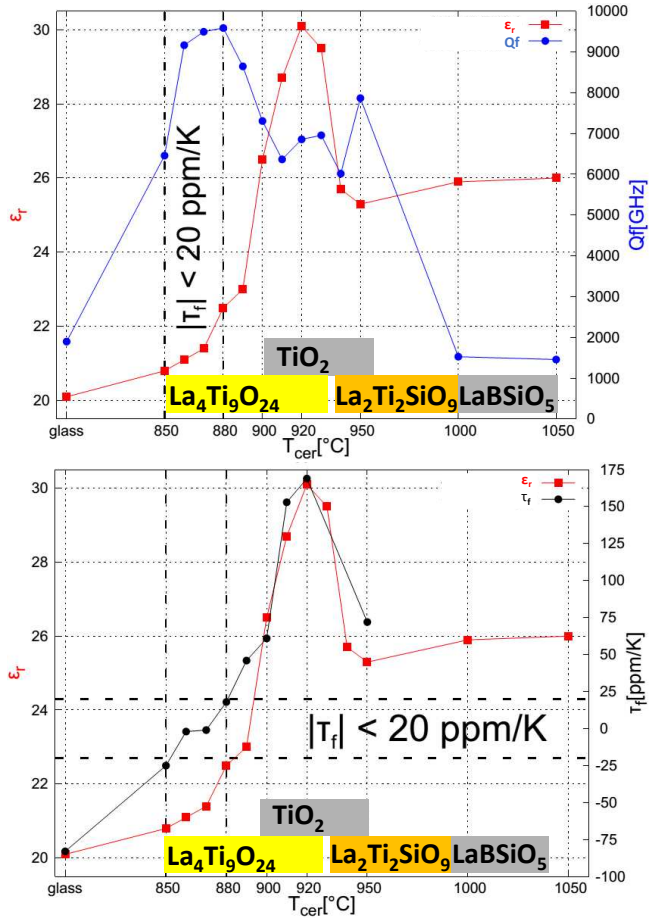

Figure 7: Dielectric properties of S1 after different ceramming temperatures (top: ε_r and Qf, bottom: ε_r and τ_f, the ceramming times vary between 5 h $< t_{\mathrm{cer}} <$ 50 h and are chosen in a way that the crystallization process in all samples is completed)

Ceramming	ε_r	Qf[GHz]	$\tan(\delta)[10^{-3}]$	τ_f[ppm/K]	f[GHz]
S1	20.4	1840	5.8	-83	10.6
870°C/50h	21.4	9500	1.1	-1	10.4
880°C/50h	22.5	9590	1.1	+18	10.2
920°C/20h	30.1	6860	1.3	+169	8.9
950°C/10h	25.3	7870	1.2	+72	9.5

Table 4: Summary of the most relevant ceramized samples of glass S1